

# Substitutional Doping of Metal Contact for Monolayer Transition Metal Dichalcogenides: a Density Functional Theory Based Study

Amithraj Valsaraj, Leonard F. Register  
and Sanjay K. Banerjee

Microelectronics Research Center and Department of  
Electrical and Computer Engineering  
The University of Texas at Austin  
10100 Burnet Road Bldg. 160, Austin, TX-78758, USA  
amithrajv@utexas.edu

Jiwon Chang  
SEMATECH

257 Fuller Road #2200  
Albany, NY-12203, USA  
jiwon.chang@sematech.org

**Abstract**—Significant roadblocks to the widespread use of monolayer transition metal dichalcogenides for CMOS-logic applications are the large contact resistance and absence of reliable doping techniques. Metal contacts that pin the Fermi level within the desired band are optimal for device applications. Here, we study substitutional doping of, and various metal contacts to, monolayer MoS<sub>2</sub> using density functional theory.

**Keywords**—transition metal dichalcogenides, substitutional doping, atom-projected density of states, *ab initio*.

## I. INTRODUCTION

Monolayer transition metal dichalcogenides (TMDs) are promising two dimensional (2D) channel materials for nanoelectronic devices. The ultrathin body ensures excellent electrostatic gate control at even nanoscale channel lengths, and, in contrast to graphene, TMDs possess sizable band gaps, which are crucial for CMOS-logic applications. However, a significant roadblock to CMOS or other devices using TMDs is large contact resistance arising from Fermi level pinning at the metal-TMD interface [1]. Metal contacts that pin the Fermi level within the desired band are desired. Alternatively, as shown by recent experimental studies, contact resistance problem can be mitigated by high electron doping of TMDs to reduce the Schottky barrier width [2], much as for conventional contacts. Here, we study substitutional doping of, and various metal contacts to, monolayer (ML) molybdenum disulfide (MoS<sub>2</sub>) using density functional theory (DFT).

## II. COMPUTATIONAL DETAILS

The DFT calculations were performed using the OPENMX code based on the linear combination of numerical atomic-orbital basis sets and pseudo potentials [3]. The local density approximation (LDA) was employed for the exchange-correlation potential as LDA has been shown to reproduce the band gap of ML MoS<sub>2</sub> well [4, 5]. The atomic relaxations were performed using a rectangular supercell ( $a = 9.48$  Å,  $b = 5.47$  Å) of ML MoS<sub>2</sub> (Fig. 1(a)). To simulate substitutional doping, we replaced a single S atom in the supercell with the Group 17

halogen atom chlorine (Cl) for *n*-type doping, and the Group 15 atom phosphorus (P) for *p*-type doping. Crystal relaxation was converged to where the Hellmann-Feynman forces on the atoms were less than 0.005 eV/Å. We calculated the band structure and atom-projected density of states (AP-DOS) for the substitutionally doped ML MoS<sub>2</sub> systems, and compared them to undoped ML MoS<sub>2</sub> results.

To model the metal contacts, we placed six atomic layers of metal atoms (with the appropriate close packing structure) on top of both substitutionally doped and undoped ML MoS<sub>2</sub> (Fig. 1(b)). An atomic relaxation then was performed with the MoS<sub>2</sub> atoms and the bottom three layers of metal atoms (nearest to TMD surface) free to move in all three spatial dimensions with the same convergence criteria as outlined for previous simulations.

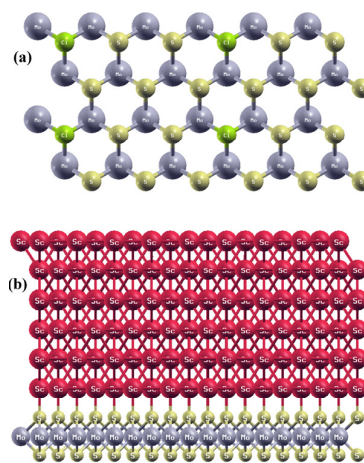


Figure 1. (a) Repeated rectangular supercells of ML MoS<sub>2</sub> used in the simulations (top view) with one Cl dopant atom (in green) replacing a single S atom in each supercell. Mo atoms are shown in blue and S atoms in gold. (b) Side view of Sc metal placed on top of Cl-doped ML MoS<sub>2</sub>.

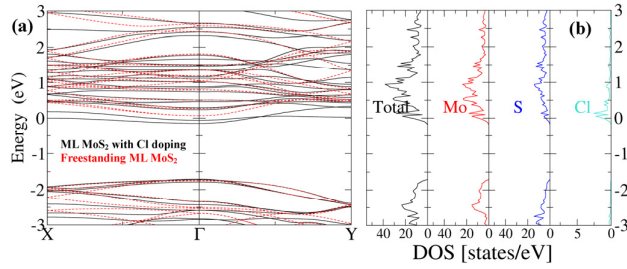


Figure 2. (a) Band structure of Cl-doped ML MoS<sub>2</sub> plotted along the high symmetry directions of the BZ (black solid lines). The Fermi level (highest occupied state more precisely) serves as the 0 eV energy reference in these 0 K simulations. The band structure of freestanding ML MoS<sub>2</sub> is superimposed for comparison (red dashed lines), although here the energy reference has been shifted in energy to provide a reasonable fit between the two band structures. (b) AP-DOS for Cl-doped ML MoS<sub>2</sub>.

### III. RESULTS

The simulated band structure of ML MoS<sub>2</sub> with Cl doping is shown in Fig. 2(a). As a rectangular supercell was utilized in our simulations, the corresponding Brillouin zone (BZ) is smaller, and ML MoS<sub>2</sub> band edges at the K point of the freestanding MoS<sub>2</sub> BZ are folded onto the  $\Gamma$  point of supercell's BZ. The zero-energy reference point for the doped system, here and below, is the highest occupied state in these 0 K simulations. The near-conduction-band-edge states are occupied or, in other words, the Fermi level is pulled into the conduction band, indicating that the ML MoS<sub>2</sub> is doped *n*-type, consistent with experiment [2]. With the large effective doping density ( $\sim 1.93 \times 10^{14} / \text{cm}^2$ ), the donor states merge with the conduction band. In addition, the AP-DOS plot (Fig. 2(b)) shows a peak for Cl atom near the conduction band edge, signifying donor states. The valence bands are largely unaffected, as shown by comparison to pure MoS<sub>2</sub> system. The zero energy reference for the latter system is adjusted to provide the best fit between the two band structures. (Otherwise, the highest occupied state energy reference would be at the valence band edge for the undoped system.)

Fig. 3(a) shows ML MoS<sub>2</sub> band structure with P doping. The near-valence-band-edge states are unoccupied or, in other words, the Fermi level is pulled into the valence band, indicating *p*-type doping. The AP-DOS plot (Fig. 3(b)) shows a peak for P atom near the valence band edge, signifying acceptor states. The conduction bands of P-doped ML MoS<sub>2</sub> remains largely unchanged, as shown by comparison to pure

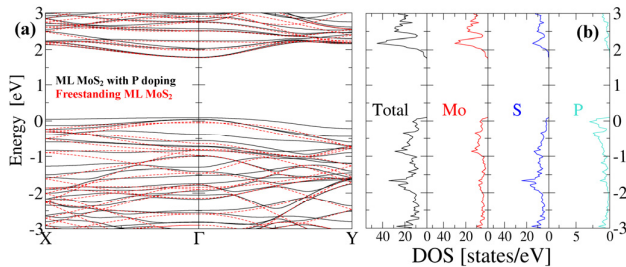


Figure 3. (a) Band structure of P-doped ML MoS<sub>2</sub> plotted along the high symmetry directions of the BZ (black solid lines). The band structure of freestanding ML MoS<sub>2</sub> is superimposed for comparison (red dashed lines). (b) AP-DOS for P-doped ML MoS<sub>2</sub>. Energy references are defined as in Fig. 2.

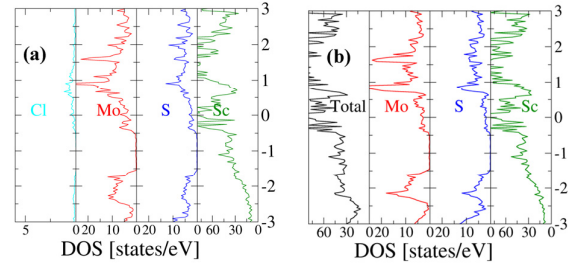


Figure 4. AP-DOS for Sc-ML-MoS<sub>2</sub> with (a) Cl-doping and (b) no substitutional doping.

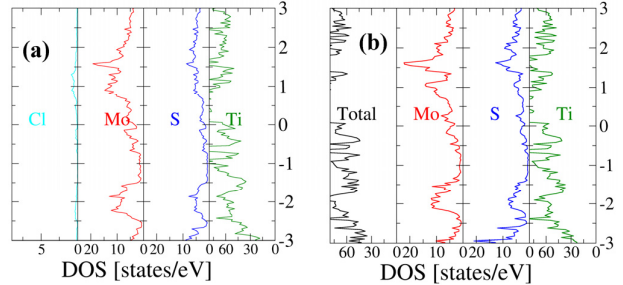


Figure 5. AP-DOS for Ti-ML-MoS<sub>2</sub> with (a) Cl-doping and (b) no substitutional doping. Note the clear “metallization” of the MoS<sub>2</sub> ML, i.e., the introduction of a significant AP-DOS within the MoS<sub>2</sub> ML into what otherwise would be the MoS<sub>2</sub> band gap.

ML MoS<sub>2</sub>.

To model metal contacts, we placed six atomic layers of either scandium (Sc), titanium (Ti), gold (Au), or silver (Ag) on top of ML MoS<sub>2</sub> with and without Cl doping and plotted the AP-DOS data for the various cases. The resulting strain in the metal was less than 0.7%. A good criterion for evaluating the metal contacts is the Schottky Barrier Height (SBH) for metal-MoS<sub>2</sub> system and the magnitude of the DOS for metal atoms near the Fermi level ( $E_F$ ).

Fig. 4(a) and (b) show the AP-DOS for Sc-MoS<sub>2</sub> ML with and without Cl doping, respectively. Similarly, partial densities of states are plotted in Fig. 5 for Ti-MoS<sub>2</sub> system. For both Sc and Ti, the Fermi level is pinned well within the conduction band, eliminating any Schottky barrier. Moreover, these metal atoms exhibit strong bonding and form interface covalent bonds with ML MoS<sub>2</sub> [5]. This bonding leads to a strong perturbation of the band structure of ML TMDs. Most evidently for Ti-ML-MoS<sub>2</sub> system, a substantial AP-DOS for the MoS<sub>2</sub> ML within the nominal band gap of the MoS<sub>2</sub> results from this coupling to the metal layer. These results suggest that Sc and Ti could function as effective *n*-type contacts for ML MoS<sub>2</sub>.

The practical application of Sc and Ti metal contacts, however, is limited due to inherent material properties. Sc is extremely reactive and requires stringent deposition conditions like very low pressure. Ti is more practical to deposit but is still prone to oxidation.

Au and Ag metal contacts are widely used experimentally as contacts for ML TMD devices [2, 7, 8]. Moreover,

experimental findings characterizing the surface morphology of metal-MoS<sub>2</sub> interfaces indicate that Au and Ag films form smoother and denser films on MoS<sub>2</sub> than Au and Ti stack do [6]. Hence, we also simulated Au and Ag metal contacts, on top of ML MoS<sub>2</sub> with and without substitutional-Cl-based *n*-type doping.

The simulated AP-DOS for MoS<sub>2</sub> with Au and Ag metal contacts are plotted in Fig. 6 and Fig. 7, respectively. Both Au and Ag exhibit medium strength bonding with ML MoS<sub>2</sub>, as evidenced by the AP-DOS in the MoS<sub>2</sub> ML within the nominal MoS<sub>2</sub> band gap. Without Cl *n*-type doping, the Fermi level is pinned very near the apparent conduction band edge with Au contacts (Fig. 6(b)) and perhaps somewhat above a broadened conduction band edge with Ag (Fig. 7(b)). With the addition of substitutional doping by Cl atoms, the Fermi level is pulled within the conduction band with either metal (Fig. 6(a) and Fig. 7(a)), suggesting their suitability as *n*-type contacts. However, the AP-DOS for the metal atom near the Fermi level with both Ag and Au contacts remains significantly smaller than it does with Sc and Ti contacts.

#### IV. CONCLUSION

Our simulation results suggest that ML MoS<sub>2</sub> can be doped *n*-type or *p*-type by substituting an S atom in the supercell with a group-17 Cl atom or a group-15 P atom, respectively. Our simulations also suggest that Sc and Ti would serve as excellent contacts to *n*-type ML MoS<sub>2</sub> due to the strong bonding and large number of states near the Fermi level. But our theoretical expectations are tempered by the material characteristics, i.e., the extremely reactive nature of Sc and the oxidation prone nature of Ti atoms. We also studied commonly used Ag and Au metal contacts to ML MoS<sub>2</sub>, which exhibited medium strength bonding to MoS<sub>2</sub> and an apparent pinning of

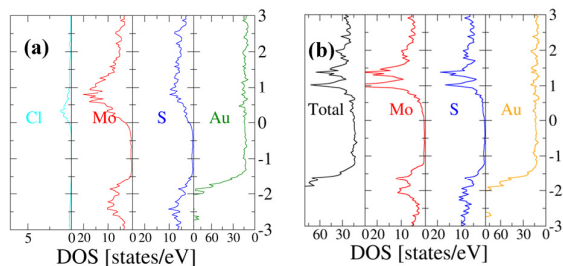


Figure 6. AP-DOS for Au-ML-MoS<sub>2</sub> with (a) Cl *n*-type doping and (b) no substitutional doping.

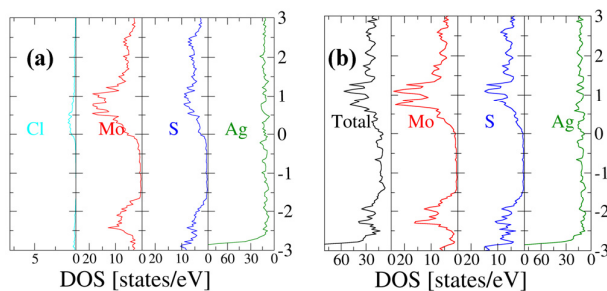


Figure 7. AP-DOS for Ag-ML-MoS<sub>2</sub> with (a) Cl *n*-type doping and (b) no substitutional doping.

the Fermi level nearer to the nominal MoS<sub>2</sub> conduction band edge. As compared with experiments, these results appear consistent with the qualitative trend for the SBH, but also optimistic overall, with Sc pinning the Fermi level ~30 meV below the conduction band edge [9], and Au pinning it ~126 meV below the conduction band edge [10]. Quantitative differences may lie in the employed DFT approach including the strained metal crystal structures required for lattice matching within a practical unit cell size, as well as in differences between the simulated and physical MoS<sub>2</sub>-metal interface, where defects and/or surface reformation and larger metal-to-surface separations in the experimental systems are possible in the latter.

#### ACKNOWLEDGMENT

This work is supported by SEMATECH, the Nanoelectronics Research Initiative (NRI) through the Southwest Academy of Nanoelectronics (SWAN), and Intel. We thank the Texas Advanced Computing Center (TACC) for computational support. A.V. would like to thank Amritesh Rai for input regarding the experimental components for ML TMD devices.

#### REFERENCES

- [1] Y. Yoon, K. Ganapathi, and S. Salahuddin, "How Good Can Monolayer MoS<sub>2</sub> Transistors Be?," *Nano Lett.*, vol. 11, no. 9, pp. 3768–3773, Sep. 2011.
- [2] L. Yang, K. Majumdar, H. Liu, Y. Du, H. Wu, M. Hatzistergos, P. Y. Hung, R. Tieckelmann, W. Tsai, C. Hobbs, and P. D. Ye, "Chloride Molecular Doping Technique on 2D Materials: WS<sub>2</sub> and MoS<sub>2</sub>," *Nano Lett.*, vol. 14, no. 11, pp. 6275–6280, Nov. 2014.
- [3] T. Ozaki and H. Kino, "Efficient projector expansion for the *ab initio* LCAO method," *Phys. Rev. B*, vol. 72, no. 4, p. 045121, Jul. 2005.
- [4] J. Chang, L. F. Register, and S. K. Banerjee, "Ballistic performance comparison of monolayer transition metal dichalcogenide MX<sub>2</sub> (M = Mo, W; X = S, Se, Te) metal-oxide-semiconductor field effect transistors," *J. Appl. Phys.*, vol. 115, no. 8, p. 084506, Feb. 2014.
- [5] J. Kang, W. Liu, D. Sarkar, D. Jena, and K. Banerjee, "Computational Study of Metal Contacts to Monolayer Transition-Metal Dichalcogenide Semiconductors," *Phys. Rev. X*, vol. 4, no. 3, p. 031005, Jul. 2014.
- [6] H. Yuan, G. Cheng, L. You, H. Li, H. Zhu, W. Li, J. J. Kopanski, Y. S. Obeng, A. R. Hight Walker, D. J. Gundlach, C. A. Richter, D. E. Ioannou, and Q. Li, "Influence of Metal-MoS<sub>2</sub> Interface on MoS<sub>2</sub> Transistor Performance: Comparison of Ag and Ti Contacts," *ACS Appl. Mater. Interfaces*, vol. 7, no. 2, pp. 1180–1187, Jan. 2015.
- [7] A. Rai, A. Valsaraj, H. C. P. Movva, A. Roy, R. Ghosh, S. Sonde, S. Kang, J. Chang, T. Trivedi, R. Dey, S. Guchhait, S. Larentis, L. F. Register, E. Tutuc, and S. K. Banerjee, "Air Stable Doping and Intrinsic Mobility Enhancement in Monolayer Molybdenum Disulfide by

- Amorphous Titanium Suboxide Encapsulation,” *Nano Lett.*, Jun. 2015.
- [8] B. Radisavljevic, M. B. Whitwick, and A. Kis, “Integrated Circuits and Logic Operations Based on Single-Layer MoS<sub>2</sub>,” *ACS Nano*, vol. 5, no. 12, pp. 9934–9938, Dec. 2011.
- [9] S. Das, H.-Y. Chen, A. V. Penumatcha, and J. Appenzeller, “High Performance Multilayer MoS<sub>2</sub> Transistors with Scandium Contacts,” *Nano Lett.*, vol. 13, no. 1, pp. 100–105, Jan. 2013.
- [10] N. Kaushik, A. Nipane, F. Basheer, S. Dubey, S. Grover, M. M. Deshmukh, and S. Lodha, “Schottky barrier heights for Au and Pd contacts to MoS<sub>2</sub>,” *Appl. Phys. Lett.*, vol. 105, no. 11, p. 113505, Sep. 2014.